Applied Mathematics, Modeling and Computer Simulation
C.-H. Chen et al. (Eds.)

doi:10.3233/ATDE221111

Legendre Polynomial Approach for Multimodal Analysis of the Transverse-Type Rectangular Piezoelectric Transformer with Common Ground Electrodes

Joli RANDRIANARIVELO[a, 1], Faniry Emilson RATOLOJANAHARY[a], Mohamed RGUITI[b], Derandraibe Jeannot FALIMIARAMANANA[a]
[a]*Université de Fianarantsoa, LAboratoire de Physique Appliquée de l'Université de Fianarantsoa (LAPAUF), Fianarantsoa Madagascar, BP 301*
[b]*Univertsité. Polytechnique Hauts-de-France (UPHF)-F-59600, France*

Abstract. A Legendre polynomial approach (PA) is proposed to forecast a thin film of transverse-type rectangular piezoelectric transformer (PT) performance with common ground electrodes located on its whole bottom surface, fabricated from a PZT5A (lead zirconate titanate) ceramic material. Based on the automatic incorporation of boundary conditions into the equations of motion and the development on a basis of orthonormal polynomials of the fields, formulations calculated analytically are simulated numerically. Then, series and parallel resonance frequencies, profiles of the mechanical displacement and the electrical potential are obtained for the PT. Our results are validated through a comparison with the three-dimensional Finite Element Method (FEM) ones. Furthermore, the mechanical tethers positions are located at the PT's junctions.

Keywords. Piezoelectric transformer, Polynomial approach, Modal analysis, Plane-stress hypothesis, Finite element method.

1. Introduction

Development of the mathematic application gives now several advantages in micro-fabrication technology. In electronic equipments, optimisations of the parameters into the devices require a modeling, design and the experimental validation in Laboratory [1]. In micro-robotic, requirements are conducted through the power density, actuation forces, operation frequencies, etc. Miniaturized piezoelectric transformers are a device permits to balance higher step frequencies with larger ranges of motion [2]. They are entirely dedicated to the galvanic isolation for DC/AC or DC/DC converter [5] and to the systems of electronic or electromechanical that requires voltage source boosted or bucked [4]. They exhibit a good efficiency at resonance over the conventional electromagnetic ones [5].

[1] Université de Fianarantsoa, LAboratoire de Physique Appliquée de l'Université de Fianarantsoa (LAPAUF), Fianarantsoa Madagascar, BP 301; Email: khicksjah@gmail.com

This work is motivated by ongoing challenges of PT with common ground electrodes (PTCGE) commercialized in monolithic micro-fabrication as presented in figure 1. Recently, approaches applied on the PTCGE are not finding the right parameters for a correct operation using either the Hamilton's principle [4] or equivalent circuit [7] model. Moreover, the FEM (finite element method) requires high storage capacity and not appear mathematic expressions [3]. In this paper, the polynomial approach (PA) which a semi-analytical method that is at time analytic and numeric is applied to study the free vibration modes of this PTCGE. It has been successfully used for Rosen-type PT [3] analyzing.

2. Structure Description

2.1. Studied PT

Figure 1 shows the studied PT with respectively L=25 mm, W=5 mm, H=1.7 mm the length, width and thickness. At the driving part, it is polarized along its thickness direction by an input voltage of amplitude V_p=1 Volt and connected to a load resistance R_L at the secondary electrodes with an output voltage V_s. The L2-L1 defines the gap. The structure is made of lead titanate zirconate (PZT5A) ceramic material and of class crystal hexagonal 6-mm. The whole bottom surfaces are completely covered with ground electrodes and different patterns of electrodes are deposited on the upper surface to create the input and output parts [6]. The x_3 direction coincides to the crystallographic Z-axis. Temporal dependence is exp(jωt), ω the angular frequency and t the time, $j^2 = -1$. Applied change of variables are: $q_1 = x_1/L$; $q_2 = 2x_2/W$; $q_3 = 2x_3/H$. We admit the normalization systems $\bar{T}_{ij}^{(R)} = T_{ij}^{(R)}/\bar{C}_{11}^{E}$ for the stress tensor where $\bar{C}_{11}^{E} = C_{11} - C_{13}^{2}/C_{33}$ and $\bar{D}_i^{(R)} = D_i^{(R)}/\varepsilon_{33}$ for the electrical displacement, R = 1, 2, 3 the region number. We assume $E_1^{(1)} = E_1^{(3)} = E_2^{(1)} = E_2^{(3)} = 0$ for the electric field components and we normalize the angular frequency as $\Omega = \omega/\omega_p$ $\omega_p = (\pi/2L)\sqrt{\bar{C}_{11}^{E}/\rho}$ is the one-dimensional thickness resonance angular frequency and ρ=7750 Kg/m3 the mass density. The elastic stiffness (N/m^2) are: $C_{11} = 12.1\ 10^{10}$; $C_{12} = 7.54\ 10^{10}$; $C_{13} = 7.52\ 10^{10}$; $C_{33} = 11.1\ 10^{10}$; $C_{66} = 2.26\ 10^{10}$

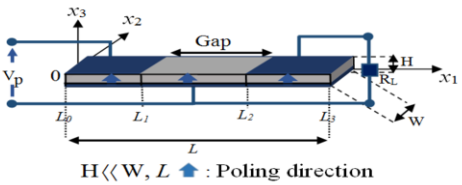

Figure 1. Piezoelectric Transformer with Common Ground Electrodes (PTCGE) description

2.2. Boundary and Continuity Conditions

The following assumptions are adopted: the thicknesses of electrodes are neglected; we suppose that the mechanical outer surfaces are mechanically free. That means:

$$u_k^{(1)}(q_1=q_p,q_2)=u_k^{(2)}(q_1=q_p,q_2);\qquad u_k^{(2)}(q_1=q_s,q_2)=u_k^{(3)}(q_1=q_s,q_2);$$

$$\Phi^{(1)}(q_1=q_p,q_2,q_3)=\Phi^{(2)}(q_1=q_p,q_2,q_3);\ \Phi^{(2)}(q_1=q_s,q_2,q_3)=\Phi^{(3)}(q_1=q_s,q_2,q_3);$$

A 2-D modeling under the plane-stress hypothesis is assumed (H⟨⟨W,L), then $T_3\langle\langle T_1, T_2$; $T_3 \approx T_4 \approx T_5 \approx 0$. Mechanical displacements u and stresses, electrical potentials Φ and displacements are continuous at the $q_1 = q_p$ and $q_1 = q_s$ interfaces, that is, $\forall\ q_2, q_3$:

$$\begin{cases} T_1^{(1)}(q_1=-1,\ q_2)=T_6^{(1)}(q_1=-1,\ q_2)=T_1^{(3)}(q_1=1,q_2)=T_6^{(3)}(q_1=1,\ q_2)=0 \\ T_2^{(R)}(q_1,q_2=\pm 1)=T_6^{(R)}(q_1,q_2=\pm 1)=0,\ \forall\ R=1,\ 2,\ 3. \end{cases}$$

3. Mathematical Resolution

Electrical field applied along the q_3 direction to the driving parts generates a mechanical deformation induces back an electric energy to the secondary electrodes [5] given by the equations of motion:

$$\begin{cases} \dfrac{\partial \bar{T}_{ij}^{S}}{\partial q_j}=-\rho\omega^2\dfrac{L}{2\bar{C}_{11}^{E}}u_i^S \\ \dfrac{\partial \bar{D}_i^{S}}{\partial q_i}=0 \end{cases} \tag{1}$$

and

$$\begin{cases} \bar{T}_{ij}^{(R)}=\dfrac{\bar{C}_{ijkl}^{,E}}{L}\left(\dfrac{\partial u_k^{(R)}}{\partial q_l}+\chi\dfrac{\partial u_l^{(R)}}{\partial q_k}\right)+f(\bar{e}_{kij}/r)\dfrac{\partial \Phi^{(R)}}{\partial q_j} \\ \bar{D}_i^{(R)}=\dfrac{\bar{e}_{ijk}^{\prime}\,r}{L}\left(\dfrac{\partial u_j^{(R)}}{\partial q_k}+\chi\dfrac{\partial u_k^{(R)}}{\partial q_j}\right)-f\bar{\varepsilon}_{ij}^{\prime}\dfrac{\partial \Phi^{(R)}}{\partial q_j} \end{cases} \tag{2}$$

with $i,j,k,l=1,2,3$; $u^S=u_i^{(1)}+u_i^{(2)}+u_i^{(3)}$. S defines the global structure. To automatically incorporate the boundary and continuity conditions into (1) and (2), the rectangular windows functions Π defined by:

$$\begin{cases} \Pi^{-1,q_p}(q_1)=\begin{cases}1,if\ -1\le q_1\le q_p\\0,otherwise\end{cases};\Pi^{q_p,q_s}(q_1)=\begin{cases}1,ifq_p\le q_1\le q_s\\0,otherwise\end{cases} \\ \Pi^{q_s,1}(q_1)=\begin{cases}1,ifq_s\le q_1\le 1\\0,otherwise\end{cases};\Pi^{-1,1}(q_2)=\begin{cases}1,if\ -1\le q_2\le 1\\0,otherwise\end{cases} \end{cases} \tag{3}$$

are used. Then, the mechanical stress and the electrical displacement are respectively:

$$\bar{T}_{ij}^{S}=\left(\bar{T}_{ij}^{(1)}\Pi^{-1,q_p}(q_1)+\bar{T}_{ij}^{(2)}\Pi^{q_p,q_s}(q_1)+\bar{T}_{ij}^{(3)}\Pi^{q_s,1}(q_1)\right)\Pi^{-1,1}(q_2) \tag{4}$$

$$\bar{D}_i^{S}=\left(\bar{D}_i^{(1)}\Pi^{-1,q_p}(q_1)+\bar{D}_i^{(2)}\Pi^{q_p,q_s}(q_1)+\bar{D}_i^{(3)}\Pi^{q_s,1}(q_1)\right)\Pi^{-1,1}(q_2) \tag{5}$$

The mechanical displacement $u_k^{(R)}$ and electrical potential $\Phi^{(R)}$ components are developed as follow:

$$u_k^{(1)}(q_1,q_2)=Q_m^{(1)}(q_1)Q_n(q_2)p_{k,mn}^{(1)}; \tag{6.a}$$

$$u_k^{(2)}(q_1,q_2)=u_k^{(1)}(q_1=q_p,q_2)+(q_1-q_p)Q_m^{(2)}(q_1)Q_n(q_2)p_{k,mn}^{(2)}; \tag{6.b}$$

$$u_k^{(3)}(q_1,q_2)=u_k^{(2)}(q_1=q_s,q_2)+(q_1-q_s)Q_m^{(3)}(q_1)Q_n(q_2)p_{k,mn}^{(3)}; \tag{6.c}$$

$$\Phi^{(1)}(q_1,q_2,q_3)=\frac{V_p}{2}(q_3+1); \tag{7.a}$$

$$\Phi^{(2)}(q_1,q_2,q_3)=\frac{(q_3+1)}{2}(q_1-q_p)(q_1-q_s)Q_m^{(2)}(q_1)Q_n(q_2)r_{mn}^{(2)} + \frac{-q_1+q_s}{q_s-q_p}\Phi^{(1)}(q_1=q_p,q_2,q_3)+\frac{q_1-q_p}{q_s-q_p}\Phi^{(3)}(q_1=q_s,q_2,q_3); \tag{7.b}$$

$$\Phi^{(3)}(q_1,q_2,q_3)=\frac{V_s}{2}(q_3+1); \tag{7.c}$$

$Q_m^{(R)}(q_1)=\sqrt{\frac{(2m+1)L}{2\left(L_R-L_{R-1}\right)}}P_m\left(\frac{q_1L}{\left(L_R-L_{R-1}\right)}-\frac{\left(L_R+L_{R-1}\right)}{\left(L_R-L_{R-1}\right)}\right)$; $L_0=0$; $Q_n^{(R)}(q_2)=\sqrt{(2n+1)/2}\,P_n(q_2)$ P_m and P_n the Legendre polynomials of degree m and n [3]; $p_{k,mn}^{(R)}$ and $r_{mn}^{(2)}$ the expansion coefficients and $k = 1, 2$. Taking into account the assumptions, (1) and (2) become:

$$\begin{cases} \left(\frac{2}{\chi}\delta_{i2}+\delta_{i1}\right)\sum_R\frac{\partial\bar{T}_{ij}^{(R)}}{\partial q_i}+\frac{2}{\chi}\delta_{2j}\sum_R\bar{T}_{ij}^{(R)}\left[\delta(q_j+1)-\delta(q_j-1)\right]- \\ \delta_{1j}\bar{T}_{ij}^{(3)}\left[\delta(q_j-1)-\delta(q_j+1)\right]+\delta_{i1}\left[\bar{T}_{ij}^{(2)}-\bar{T}_{ij}^{(1)}\right]\delta(q_i-q_p)+ \\ \delta_{i1}\left[\bar{T}_{ij}^{(3)}-\bar{T}_{ij}^{(2)}\right]\delta(q_i-q_s)=-\left(\pi^2\Omega^2/4\right)\sum_R u_j^{(R)} \\ \frac{\partial\bar{D}_1^{(2)}}{\partial q_1}+\chi\frac{\partial\bar{D}_2^{(2)}}{\partial q_2}+\chi\bar{D}_2^{(2)}\left(\delta(q_2+1)-\delta(q_2-1)\right)-f\bar{D}_3^{(2)}\delta(q_3-1)=0 \end{cases} \tag{8}$$

$$\bar{T}_1^{(R)}=\frac{2}{L}\left\{\bar{C}_{11}\frac{\partial u_1^{(R)}}{\partial q_1}+\chi\bar{C}_{12}\frac{\partial u_2^{(R)}}{\partial q_2}+f\left(\bar{e}_{31}/r\right)\frac{\partial\Phi^{(R)}}{\partial q_3}\right\} \tag{9.a}$$

$$\bar{T}_2^{(R)}=\frac{2}{L}\left\{\bar{C}_{12}\frac{\partial u_1^{(R)}}{\partial q_1}+\chi\bar{C}_{11}\frac{\partial u_2^{(R)}}{\partial q_2}+f\left(\bar{e}_{31}/r\right)\frac{\partial\Phi^{(R)}}{\partial q_3}\right\} \tag{9.b}$$

$$\bar{T}_6^{(R)}=\frac{2}{L}\bar{C}_{66}\left\{\frac{\partial u_2^{(R)}}{\partial q_1}+\chi\frac{\partial u_1^{(R)}}{\partial q_2}\right\} \tag{9.c}$$

$$\bar{D}_1^{(R)}=-\frac{2}{L}\bar{\varepsilon}_{11}\left\{\frac{\partial\Phi^{(R)}}{\partial q_1}\right\} \tag{10.a}$$

$$\bar{D}_2^{(R)}=-\frac{2}{L}\chi\bar{\varepsilon}_{11}\left\{\frac{\partial\Phi^{(R)}}{\partial q_2}\right\} \tag{10.b}$$

$$\bar{D}_3^{(R)}=\frac{2}{L}\left\{\bar{e}_{31}r\frac{\partial u_1^{(R)}}{\partial q_1}+\chi\bar{e}_{31}r\frac{\partial u_2^{(R)}}{\partial q_2}-f\bar{\varepsilon}_{33}\frac{\partial\Phi^{(R)}}{\partial q_3}\right\} \tag{10.c}$$

with: $\bar{C}_{11}=(C_{11}-(C_{13}^2/C_{33}))/\bar{C}_{11}^E$; $\bar{C}_{66}=C_{66}/\bar{C}_{11}^E$; $r=10^{-10}\sqrt{\bar{C}_{11}^E/\varepsilon_{33}}$; $\bar{C}_{12}=(C_{12}-(C_{13}^2/C_{33}))/\bar{C}_{11}^E$; $\bar{\varepsilon}_{11}=\varepsilon_{11}/\varepsilon_{33}$; $\bar{\varepsilon}_{33}=1+e_{33}^2/(\varepsilon_{33}C_{33})$; $\bar{e}_{31}=(e_{31}-(C_{13}/C_{33})e_{33})/\sqrt{\varepsilon_{33}\bar{C}_{11}^E}$; $e_{31}=-5.4; e_{33}=15.8$: piezoelectric constants (C/m2), $\varepsilon_{11}=916$; $\varepsilon_{33}=830$: relative permittivity (F/m); $f=L/H$: form factor and $\chi=W/H$:

The terms $\delta_{2j}\bar{T}_{ij}^{(R)}\left[\delta(q_j\pm1)\right]$; $\delta_{1j}\bar{T}_{ij}^{(3)}\left[\delta(q_j-1)\right]$; $\delta_{1j}\bar{T}_{ij}^{(1)}\left[\delta(q_j+1)\right]$, in (8) ensure that $\bar{T}_{i1}^{(1)}=\bar{T}_{i1}^{(3)}=\bar{T}_{2j}^{(R)}=0$ and $\bar{D}_2^{(2)}=0$ at the mechanically free surfaces. At $q_1=q_s$ and $q_1=q_p$, the continuity of stresses is introduced respectively by the terms $\delta_{i1}\left[\bar{T}_{ij}^{(3)}-\bar{T}_{ij}^{(2)}\right]\delta(q_i-q_s)$; $\delta_{i1}\left[\bar{T}_{ij}^{(2)}-\bar{T}_{ij}^{(1)}\right]\delta(q_i-q_p)$. In region 2, $\bar{D}_3^{(2)}$ = constant along the q_3

direction is introduced by the $\overline{D}_3^{(2)}\delta(q_3-1)$ term. In Eq. 8, substituting the $u_k^{(R)}$ and $\Phi^{(R)}$ by their expressions and after having multiplied by $Q_j^*(q_1)$ and $Q_k^*(q_2)$, by integrating over q_1 from -1 to q_p, q_p to q_s, q_s to 1 and over q_2 from -1 to 1 in region R, leads to a system of matrix equation (11).

$$AA * P + J * V_S = -(\pi^2\Omega^2/4)CC * P - A * V_p \quad (11)$$

Where $P = \left[p_{1,mn}^{(1)}, p_{2,mn}^{(1)}, p_{1,mn}^{(2)}, p_{2,mn}^{(2)}, p_{1,mn}^{(3)}, p_{2,mn}^{(3)} \right]^T$ is the unknown vector. T denotes a transposed matrix. A, AA, CC, J are the matrices with m lines and n columns.

4. Analytical Results - Multimodal Analysis

The series resonance frequencies Ω_r are obtained by vanishing the load resistance (R_L = 0) and letting the driving electrodes short circuited (V_p=0). The equation (11) becomes:

$$CC^{-1} * AA * P = -\frac{\pi^2\Omega_r^2}{4} * I_d * P. \quad (12)$$

Besides, by short-circuiting the input part, we get the parallel resonance frequencies Ω_a allowing the receiving electrodes open (i_S=0). From (11), we have (13) where Id denotes the identity matrix.

$$CC^{-1} * MM * P = -\frac{\pi^2\Omega_a^2}{4} * I_d * P. \quad (13)$$

5. Numerical Simulation

5.1 PA Convergence

Summation over *m* and *n* is numerically truncated to the finite values M and N respectively. The PA convergence is reached for M and N increased with no variations of the frequencies values. Presented in tables 1 and 2, the first 4 modes convergence is obtained from the orders of truncation M = N = 10.

Table 1. Resonance frequencies

	2D $f_{r,PA}$ (*10^{5}Hz)			
Orders of truncation	**Mode 1**	**Mode 2**	**Mode 3**	**Mode 4**
M=N=3	0.5717	1.1350	1.6398	2.1397
M=N=7	0.5855	1.1339	1.6651	2.1175
M=N=10	0.5863	1.1340	1.6647	2.1174
M=N=12	0.5863	1.1340	1.6647	2.1174
M=N=15	0.5863	1.1340	1.6647	2.1174
3D $f_{r,FEM}$ (*10^{5}Hz)	0.5865	1.1337	1.6622	2.1160
ε_{fr} (%)	0.0341	0.0265	0.1502	0.0661

Table 2. Anti-resonance frequencies

	2D $f_{a,PA}$ (*10^{5}Hz)			
Orders of truncation	**Mode 1**	**Mode 2**	**Mode 3**	**Mode 4**
M=N=3	0.5786	1.1501	1.6526	2.1402
M=N=7	0.5893	1.1493	1.6814	2.1213

M=N=10	0.5900	1.1494	1.6812	2.1214
M=N=12	0.5899	1.1494	1.6812	2.1214
M=N=15	0.5899	1.1494	1.6812	2.1214
3D $f_{a,\,FEM}$ (*10^5Hz)	0.5905	1.1498	1.6783	2.1197
ε_{fa} (%)	0.1016	0.0348	0.1728	0.0801

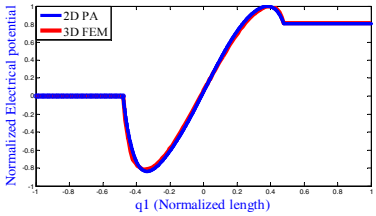

Figure 2. Normalized electrical potentials

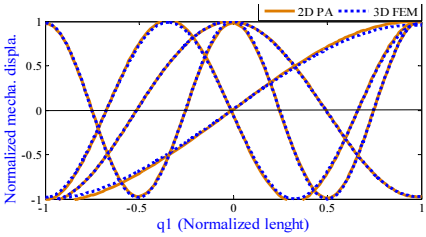

Figure 3. Normalized mechanical displacements

5.2 Validation of the Model and Discussion

The resonance *fr* and anti-resonance *fa* frequencies of the first four modes found from the 2D PA and 3D FEM are given in tables 1 and 2. The relative errors are calculated as follows:

$$\varepsilon_{fr} = 100 * \left| \left(f_{r,\,FEM} - f_{r,\,PA} \right) / f_{r,\,FEM} \right| \quad (14.a)$$

$$\varepsilon_{fa} = 100 * \left| \left(f_{a,\,FEM} - f_{a,\,PA} \right) / f_{a,\,FEM} \right| \quad (14.b)$$

5.3 Illustration

It is essential to predict the expressions of the fields to locate the mechanical tethers at the nodal points [3], of the operating resonance mode to maintain the PT's performances. The expressions of the mechanical displacements are obtained from the coefficients of the vectors $p_{k,mn}^{(R)}$ given by the simulation. As presented in figure 2 and 3, the second mode meets a zero value at the interfaces of the structure. It is confirmed that the mechanical stresses are continuous at qp and qs interfaces. Results obtained for both PA/FEM are in good agreement. In addition, the second mode of mechanical stress (figure 4) gives a maximum at the interfaces. The mechanical tethers should applied at these junctions. Sufficient functioning mode is the second longitudinal mode so that all vibrations give some energy density for the PT [3].

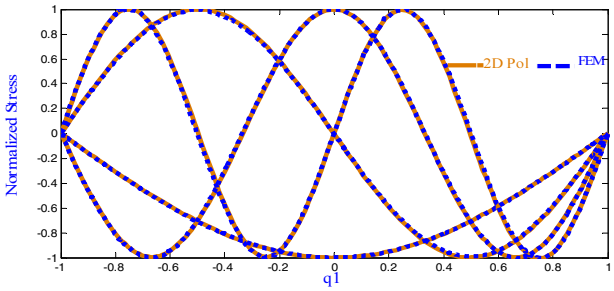

Figure 4. Normalized mechanical stress vs normalized length

A quite good agreement is found of the operating frequency with modal relative errors well below 1%. In opened-circuit case, figures 3 and 4 present respectively the profiles of the normalized mechanical displacements and electrical potentials. Results obtained with the PA approach are strongly matched with those found with the 3D FEM. Predicted boundary and continuity conditions are verified. These results validate our proposed polynomial approach.

6. Conclusion

A mathematical development using the Legendre polynomial functions for modeling the transverse-type PT has been reported based on the plane-stress hypothesis. Results found with the 2D PA are validated and agree very satisfactorily with the 3D FEM results. Boundary and continuity conditions are verified. PA allows for locate the mechanical tethers of the transformer. In the future work, the frequency's and load's dependence in the electrical behaviours of the PT are in progress as well as the experimental validation in order to confirm our simulation results.

References

[1] F. Boukazouha, F. Boubenider, Guylaine P. Vittrant, L. P. Tran-Huu-Hue, Marc L., M. Rguiti, “Parameter Determination of a Rosen Type Piezoelectric Transformer Operating in Second Mode,” IEEE, 4th International Conference on Power Elgineering, Energy and Electrical Drives, Istanbul, Turkey, pp. 485-489, May 13-17, 2013..

[2] M. Shin, J. Choi, R. Q. Rudy, C. Kao, J. S. Pulskamp, R. G. Polcawich, Oldham, “Micro-Robotic actuation units based on thin-Film Piezoelectric and High-aspect ratio Polymer Structures,” Proceedings of the ASME 2014 International Design Engineering Technical Conference & Computers and Information in Engineering Conference, Buffalo. New York. USA, August 2014.

[3] D. J. Falimiaramanana, F. E. Ratolojanahary, J. E. Lefebvre, L. Elmaimouni, M. Rguiti, “2D Modeling of Rosen-type piezoelectric transformer by means of a polynomial approach,” IEEE transactions on ultrasonics, ferroelectrics, and frequency control, vol. 67, no. 8, pp. 1701-1720, august 2020.

[4] O. M. Barham, M. Mirzaeimoghri, and D. L. DeVoe, “Piezoelectric Disc Transformer Modeling Utilizing Extended Hamilton’s Principle,” IEEE, vol. 0885-8993, pp. 1-10.

[5] D. Vasic, F. Costa, E. Sarraute, “A new method to design Piezoelectric transformer used in MOSFET/IGBT Gate Drive Circuits, ” unpublished.

[6] Y. Zhuang, Seyit O. Ural, R. Gosain, S. Tuncdemir, A. Amin, K. Uchino, “High Power PT with Pb(Mg1/3Nb2/3)O3-PbTiO3 Single Crystals,” Appl. Phys. Express 2, vol. 121402, 2009.

[7] J. Yang, J. Liu, membre, IEEE and J. Li, “Analysis of a Rectangular Ceramic Plate in Electrically Forced Thickness-Twist Vibration as a Piezoelectric Transformer,” IEEE transactions on ultrasonics, ferroelectrics, and frequency control, vol. 54, No. 4, pp. 830–835, April 2007.